SEMI-TWInS: Simultaneous Extraction of Myelin and Iron using a T_2*-Weighted Imaging Sequence

F. Schweser[1,2], A. Deistung[1], B. W. Lehr[3], K. Sommer[1,4], and J. R. Reichenbach[1]

[1]Medical Physics Group, Dept. of Diagnostic and Interventional Radiology 1, Jena University Hospital, Jena, Germany, [2]School of Medicine, Friedrich Schiller University of Jena, Jena, Germany, [3]Medical Physics Group, Dept. of Diagnostic and Interventional Radiology, Jena University Hospital, Jena, Germany, [4]School of Physics and Astronomy, Friedrich Schiller University of Jena, Jena, Germany

INTRODUCTION – Regional quantitative information of the non-heme iron concentration is supposed to bear enormous potential for early clinical diagnosis and monitoring of both disease and treatment and disease progression in various neurological and psychiatric disorders, such as Morbus Alzheimer or Morbus Parkinson. Quantitative magnetic susceptibility mapping (QSM) is regarded to become the first clinically applicable technique for quantitative iron mapping *in vivo*. However, the relative contribution of iron to the total bulk voxel susceptibility is contentious[1-3], especially in the presence of significant portions of potentially diamagnetic myelin. Therefore, the separation of iron and myelin is of utmost importance for clinical applicability of QSM.

In this contribution, we present, for the first time, a unique approach for quantitative whole-brain mapping of iron and myelin concentrations *in vivo* based on conventional gradient echo (GRE) data, referred to as SEMI-TWInS.

THEORY – SEMI-TWInS employs two fundamental assumptions on the relation between the effective transverse relaxation rate R_2^*, voxel bulk magnetic susceptibility χ, storage iron concentration c_{Fe}, and myelin concentration c_{My}. First, it is assumed that both R_2^* and χ depend linearly on c_{Fe} and c_{My}, i.e. $R_2^*(c_{My}, c_{Fe}) \approx a_1 \cdot c_{Fe} + a_2 \cdot c_{My} + a_3$ (1) and $\chi(c_{Fe}, c_{My}) \approx b_1 \cdot c_{Fe} + b_2 \cdot c_{My} + b_3$ (2). This assumption is based on the fact that myelin has a significant R_2^* effect[4]. Second, it is assumed that the coefficients (a_1, a_2, a_3, b_1, b_2, b_3) are equal for all types of brain tissue and independent on the patient under investigation. The coefficients may, therefore, be determined in offline calibration experiments which involve measuring of R_2*, χ, c_{Fe}, and c_{My} in several different tissue regions, followed by solving Eqs. (1) and (2) for all regions with respect to the six coefficients. Having determined the coefficients it is possible to calculate c_{Fe} and c_{My} voxel-wise from measurements of R_2^* and χ by combining Eqs. (1) and (2).

MATERIALS & METHODS

Data Acquisition and Pre-Processing: High-resolution double-echo GRE data of the whole brain were acquired from two healthy volunteers (A,B; 26y) with the ToF-SWI sequence[5] (TE_1/TE_2=3.4ms/22ms, TR/FA/BW_2=30ms/20°/80Hz/px, voxel size 600×600×600µm³, 75% partial Fourier phase/slice) on a 3T MR-scanner (Tim Trio, Siemens Medical Solutions). The acquisition was repeated twice with the volunteers' heads tilted around the left-right axis by approximately -50° and +30°. Multi-channel phase images were combined using uniform sensitivity reconstruction[6], and the SHARP method[7] was applied. For volunteer A, magnetization transfer saturation (MTS) images, representing the spatial myelin concentration (MTS $\propto c_{My}$), were generated as proposed by Helms et al.[8] (voxel size 600×600×1800µm³). All data sets were registered using FLIRT[9]. R_2^* maps were computed from the two magnitude images of the ToF-SWI data, and averaged over the three rotations. Susceptibility maps were computed from the three rotated GRE phase images as described by Schweser et al.[7].

a_1 (Hz·100g/mg)	1.5±0.2
a_2 (Hz/MTS)	3±4
a_3 (Hz)	2±13
b_1 (ppm·g/mg)	1.27±0.15
b_2 (ppm/MTS)	-0.04±0.02
b_3 (ppm)	0.12±0.08

TABLE 1. Calibration coefficients.

Calibration: The calibration coefficients were determined from volunteer A. For this purpose, mean MTS, R_2^*, and χ values were determined in ten brain regions. Using corresponding putative c_{Fe} values from a *post mortem* study by Hallgren and Sourander[10], and setting c_{My} = MTS, the six coefficients, (a_1, a_2, a_3, b_1, b_2, b_3), were calculated from Eqs. (1) and (2) using a least squares solver.

Calculation of Myelin and Iron Maps: Iron and myelin maps were computed for both volunteers solely based on the individual GRE data, i.e. R_2* and χ maps, by solving for each voxel Eqs. (1) and (2) with respect to c_{Fe}, and c_{My}.

RESULTS – The determined calibration coefficients are listed in Table 1. Figure 1 depicts representative slices of the susceptibility map (1st column), R_2* map (2nd column), iron map (3rd column), and myelin map (4th column) of volunteer B showing the thalamostriate area (first row), mesencephalon (second row), and motor cortex (third row). The calculated maps demonstrate exquisite quantitative local anatomical contrast. The iron contrast appears similar to the R_2* contrast, reflecting the notion that R_2* is a good measure for tissue iron content. However, the contrast differs in some regions (green arrows in Fig. 1b,c). The myelin map represents the myelin-induced susceptibility (b_2·MTS), and demonstrates contrast significantly different from both the iron map and the χ map (blue arrows in Fig. 1a,c,d). Significant contrast exists between GM and WM (Fig. 1l) and in regions of the corticospinal tract (red arrows in Fig. 1d,h), reflecting the increased myelin content in these regions.

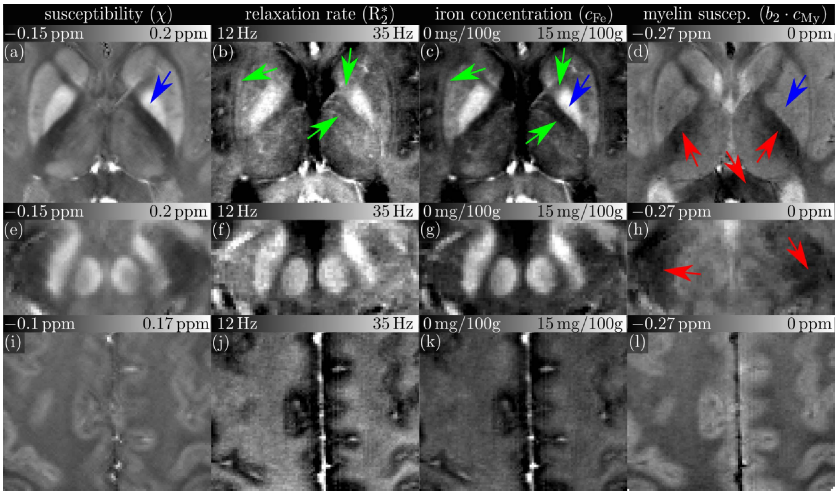

FIGURE 1. Representative slices (mean value projections over three adjacent slices) of the susceptibility map (a,e,i), R_2* map (b,f,j), iron map (c,g,k), and myelin susceptibility (d,h,l).

DISCUSSION & CONCLUSIONS – SEMI-TWInS enables quantitative mapping of both iron and myelin concentration with high resolution using conventional double-echo GRE data. Regarding the calibration coefficients, it is striking that b_1 is exactly equal to the proportionality factor between susceptibility and tissue ferritin concentration theoretically estimated by Schenck[11]. Furthermore, b_2 is negative, representing the diamagnetic properties of myelin[3]. It has to be noted, that due to the different relaxation properties compared to parenchyma, voxel values in regions with CSF and blood vessels cannot be expected to be reasonable (cf. second assumption). In this study, QSM was applied using GRE acquisitions at multiple orientations of the head in order to avoid artifacts in the susceptibility map. However, QSM may also be performed based on only a single GRE acquisition[12,13], allowing to apply the method in clinical routine where GRE sequences have already been established for generating SWI venograms[14]. Since the relation in Eq. (1) is a first-order approximation of the multi-exponential decay, it may be expected that calibration coefficients strongly depend on the chosen GRE echo times, and the usage of more than two echoes might be beneficial. In future, validation measurements are required, including investigations on the validity of Eqs. (1) and (2), and improvements of the calibration coefficients using *post mortem* iron quantification and *in vivo* FDRI-based[15] iron estimates.

REFERENCES – [1] Fukunaga M, et al. *Proc Natl Acad Sci U S A*. 2010;107(8):3834-9. [2] He X and Yablonskiy DA. *Proc Natl Acad Sci U S A*. 2009;106(32):13558-63. [3] Duyn JH et al. *Proc Natl Acad Sci U S A*. 2007;104(28):11796-801. [4] Du YP et al. *Magn Reson Med*. 2007;58(5):865-70. [5] Deistung A et al. *J Magn Reson Imaging*. 2009;29(6):1478-84. [6] Ros C et al. *ECIFMBE 2008, IFMBE Proceedings 22*. 2009:803-6. [7] Schweser F, et al. *NeuroImage* (in press). [8] Helms G, et al. *Reson Med*. 2008;60(6):1396-407. [9] Jenkinson M, et al. *NeuroImage*. 2002;17(2):825-41. [10] Hallgren B and Sourander P. *J Neurochem*. 1958;3:41-51. [11] Schenck JF. *Ann N Y Acad Sci*. 1992;649:285-301. [12] Schweser F, et al. *Med Phys*. 2010;37(9):5165-78. [13] de Rochefort L, et al. *Magn Reson Med*. 2010;63(1):194-206. [14] Reichenbach JR and Haacke EM. *NMR Biomed*. 2001;14(7-8):453-67. [15] Bartzokis G, et al. *Am J Neuroradiol*. 1994;15(6):1129-38.